

# Enhancing Weak Optical Signals Using a Plasmonic Yagi–Uda Nanoantenna Array

Evgeny G. Mironov, *Student Member, IEEE*, Abdul Khaleque, Liming Liu, Ivan S. Maksymov, and Haroldo T. Hattori, *Senior Member, IEEE*

**Abstract**—Nanoantennas have been used in a wide range of applications in sensing, spectroscopy, and imaging—in general, the antennas can enhance physical phenomena such as the local electric field or concentrate light in a certain direction. We have fabricated an array of 80 plasmonic Yagi–Uda nanoantennas on the cladding of an optical fiber and, by doing this, we show that the signal reaching the fast detector can be increased by a factor of 5 dB. The experiment demonstrates that plasmonic directive nanoantennas can indeed collect and concentrate electromagnetic radiation along a certain direction and eventually could be used to enhance weak signals.

**Index Terms**—Plasmonics, nano-antennas, fiber laser.

## I. INTRODUCTION

ANTENNAS have been used to convert a guided wave into a ‘free-space’ propagating wave and vice-versa [1]. In recent years, miniature antennas have been developed at optical frequencies, in many cases, mimicking existing radio-frequency antennas such as dipole, bow-tie, horn and Yagi-Uda antennas. The so-called nano-antennas are capable of enhancing different photo-physical processes (e.g. enhancing the local electric field) and are being used in a multitude of applications in sensing, imaging, light emission and photo-voltaic applications [2], [3].

Electromagnetic fields at the surface of metallic nanoparticles, which form the antennas, are localized and depend on the geometry of the particles – hence, it is challenging to control their radiation pattern in the far-field. However, the far-field pattern can be engineered by tailoring the properties of the antenna. For instance, Yagi-Uda nano-antennas, which borrow their name and operation principle from well-known radio-frequency counterparts [2], [4]–[8], can radiate light

preferably along a certain direction, and could find applications in bi-stable devices, nano-focusing of light, particle manipulation, optical interconnects and coupling light from free-space into a waveguide [4]. In addition to Yagi-Uda nano-antennas, other nano-antennas can lead to high directivity [9]–[12] such as a plasmonic nanowire [10], a honeycomb-like antenna structure [11] or a dipole placed close to a ring reflector [12].

Nano-antennas can be fabricated at the end of the fiber [13] or on the fiber cladding: given that nano-antennas are tiny and cannot handle high fluence [14], fabricating them on the fiber cladding allows a better control of the amount of fluence that reaches the antennas, thereby avoiding their obliteration. In addition to that, metallic structures at the end of the fiber can act as mirrors and reflect light back to the laser cavity, where it can lead to instabilities in the laser operation. Finally, the nanostructures are placed on the cladding of the fiber to study the effects of the antennas on the enhancement of weak signals.

In this letter, we have initially fabricated plasmonic nano-antennas on the fiber cladding, and then spliced the optical fiber with nano-antennas to a ring fiber laser. We show that the positioning of the nano-antennas on the fiber cladding increased the amount of power reaching the fast detector when compared with a bare fiber, and that the coupled signal through the antennas is a replica of the original signal passing through the fiber core.

## II. FABRICATION OF THE DEVICES

The fiber used in the experiments is the commercial *HI 1060* optical fiber from Corning glass: it is designed to work at wavelengths above 980 nm, with a mode-field-diameter of 6.2  $\mu\text{m}$  at 1060 nm and cladding diameter of 125  $\mu\text{m}$ . Initially, the fiber jacket is stripped and the fiber is cleaned with ethanol and immersed into an ultrasonic bath. Secondly, Focused Ion Beam (*FIB*) milling system is used at high current to remove a large area of the fiber cladding: the distance between the fiber core and the Yagi-Uda antennas is estimated to be around 50  $\mu\text{m}$ . Thirdly, 100 nm of gold is deposited on the fiber cladding and Yagi-Uda nano-antennas are fabricated by using *FIB*, as shown in Fig. 1.

The thickness of the each element of the nano-antennas is 100 nm and has a length of 70 nm. The center-to-center separation between adjacent elements is about 250 nm. The widths of the elements are: large reflector –450 nm, feeding element –300 nm and the 3 directors –150 nm. The dimensions have been optimized for operation at  $\lambda = 1060$  nm and designed

Manuscript received June 19, 2014; revised August 20, 2014; accepted August 24, 2014. Date of publication August 28, 2014; date of current version October 20, 2014. This work was supported by the Australian National Fabrication Facility for the fabrication of Yagi-Uda nanoantennas. The work of I. S. Maksymov was supported by the University Post-Doctoral Research Fellowship Scheme, University of Western Australia, Crawley, WA, Australia.

E. G. Mironov is with the School of Engineering and Information Technology, University of New South Wales, Canberra, ACT 2610, Australia, and also with the Department of Electronic Materials Engineering, Research School of Physics and Engineering, Australian National University, Canberra, ACT 0200, Australia (e-mail: e.mironov@adfa.edu.au).

A. Khaleque, L. Liu, and H. T. Hattori are with the School of Engineering and Information Technology, University of New South Wales, Canberra, ACT 2610, Australia (e-mail: abdul.khaleque@student.adfa.edu.au; liming.liu@student.adfa.edu.au; h.hattori@adfa.edu.au).

I. S. Maksymov is with the School of Physics, University of Western Australia, Crawley, WA 6009, Australia (e-mail: ivan.maksymov@uwa.edu.au).

Color versions of one or more of the figures in this letter are available online at <http://ieeexplore.ieee.org>.

Digital Object Identifier 10.1109/LPT.2014.2352339

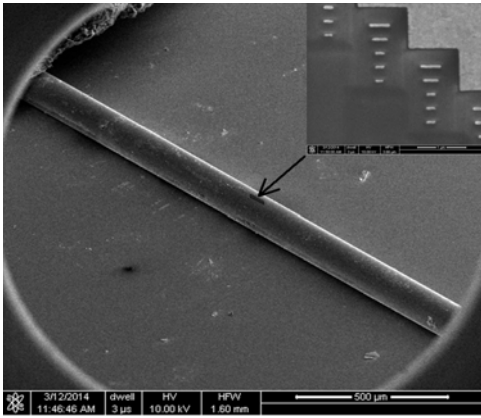


Fig. 1. Scanning Electron Microscope (SEM) image of the fabricated Yagi-Uda antennas on the optical fiber.

by using three-dimensional finite-difference time-domain (*3D FDTD*) method. The thickness is chosen so that the metal adheres well to the fiber and, at the same time, fabrication of the structures does not require extensive efforts.

Commercial *3D FDTD* software (*RSOFT FullWAVE*) [15] is used in our simulations. The grid sizes are chosen as  $\Delta x = \Delta y = \Delta z = 20$  nm, which are further refined to 5 nm close to the edges of the metallic structures. The refractive index of the cladding is assumed to be 1.45, while gold is simulated as a dispersive medium with multiple resonances [14], [15]. A Gaussian source is launched at the fiber cladding to simulate light coming from the fiber, with a spot-size of  $2 \mu\text{m}$  by  $500$  nm (vertical direction). The time-step is about  $5 \times 10^{-18}$  s, well below the Courant limit. In the simulations, the main electric field is along the  $x$ - $z$  plane ( $E_x$ ,  $E_z$ ) of the structure, the magnetic field is perpendicular to the  $x$ - $z$  plane ( $H_y$ ) [16] and the computation boundaries are terminated by perfectly matching layers.

The dimension of the feeding element aims to maximize the electric field at the edge of the element and, consequently, the electric polarizability of the antenna. The electric polarizability ( $\alpha$ ) of a rectangular particle is given by [17]:

$$\alpha \approx \frac{V}{\left(L_{feed} + \frac{\epsilon_m}{\epsilon - \epsilon_m}\right) + A\epsilon_m x^2 + B\epsilon_m^2 x^4 - j\frac{4}{3}\frac{\pi^2 \epsilon_m^{1.5} V}{\lambda_0^3}}$$

where  $L_{feed}$  is the depolarization factor,  $A(L_{feed}) = -0.4865L_{feed} - 1.046L_{feed}^2 + 0.8481L_{feed}^3$ ,  $B(L_{feed}) = 0.01909L_{feed} + 0.1999L_{feed}^2 + 0.6077L_{feed}^3$ ,  $\epsilon$  and  $\epsilon_m$  are the relative permittivities of the metallic nanoparticle the surrounding medium respectively,  $V$  is the volume of the metallic nanoparticle and  $\lambda_0$  is the wavelength in vacuum. The parameter  $x$  is defined as  $x = \pi W_{feed}/\lambda_0$  and the formula for  $L_{feed}$  can be found in [17]. The initial value of  $W_{feed}$  aims to optimize  $\alpha$  and its theoretical value is confirmed by *3D FDTD* simulations, leading to an optimized value of  $W_{feed} = 300$  nm.

Eighty (80) Yagi-Uda nano-antennas are fabricated on the fiber cladding, with each antenna being separated from a neighboring one by  $1 \mu\text{m}$  (center to center distance). The antennas are pointing at an angle ( $\phi$ ) of 135 degrees

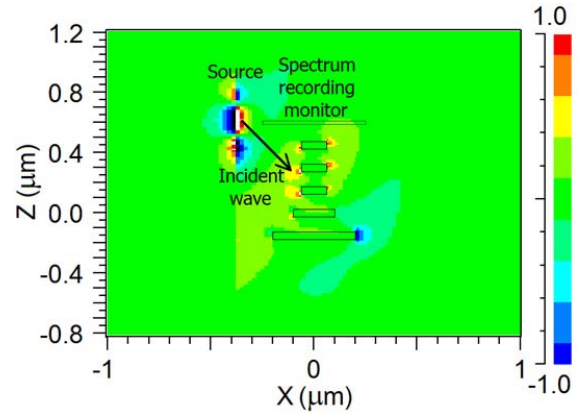


Fig. 2. Electric field ( $E_x$ ) distribution of the nano-antenna.

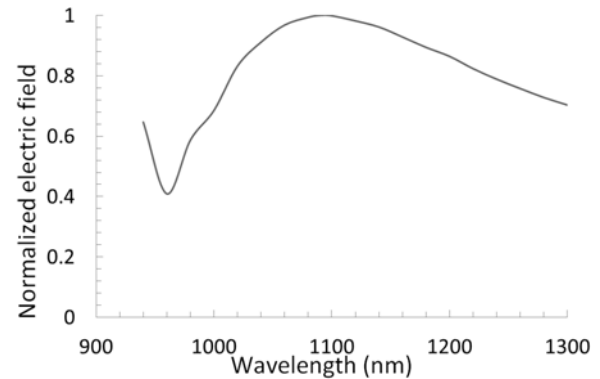


Fig. 3. Electric field ( $E_x$ ) spectrum of the Yagi-Uda nano-antenna.

(see Fig. 4 for details) to reduce the interference from the signal propagating in the forward direction in the fiber core and the one that will eventually exit at the fiber end. Otherwise, the measurement of the signal coming out from the antennas would be mixed with the strong signal leaving the fiber core.

While this approach reduces the coupling of light into the Yagi-Uda antennas, it allows a clear detection of the signal coming from the antennas. Fig. 2 ( $x$ - $z$  plane where the Yagi-Uda antenna lies) shows that coupling of light into a Yagi-Uda nano-antenna can occur even when the incident field is not aligned with the axis of the antenna. Yagi-Uda nano-antennas can capture the incident light and redirect it forward, since the antenna is highly directive: the reflector reduces the amount of light going into the rear direction, while the feed and directors concentrate the coupled light mostly in the forward direction as seen in Fig. 2.

The spectral response of the Yagi-Uda nano-antenna (Fig. 3) is obtained by placing an electric field ( $E_x$ ) monitor in front of the Yagi-Uda nano-antenna as shown in Fig. 2. The electric field is normalized with respect to its maximum value: it is clear that the antenna can operate in the wavelength range between 1000 nm and 1300 nm without significantly reducing its efficiency.

### III. EXPERIMENTAL RESULTS

In the experiments the optical ring laser shown in the schematic in Fig. 4(a) is used. The laser is pumped by

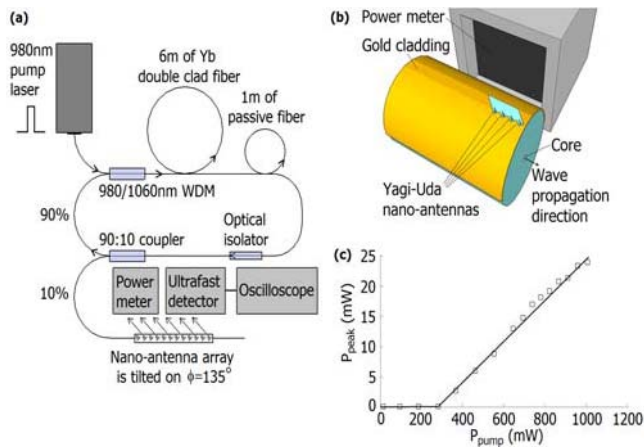


Fig. 4. (a) Schematic of the fiber laser setup, (b) sketch of the measurement setup and (c) peak power exiting the optical fiber patch spliced to the 10% arm of the 90:10 coupler versus the pump power.

a 980 nm CW laser that can be externally modulated at a maximum repetition rate of 3 kHz and has a maximum peak power of 1.5 W. The pump light is coupled into a WDM coupler, which allows light to get into the ytterbium (Yb) doped fiber, but prevents a reflected beam at 1091 nm to return to the pump laser. The Yb doped fiber has a double cladding that allows the pump beam to propagate in the inner cladding and be absorbed by the fiber core, while the emitted signal propagates mostly through the fiber core.

The additional meter of passive fiber helps to dump the remaining pump power that is not absorbed by the fiber core. The generated light, at the free-space wavelength of 1091 nm, then goes through an optical isolator to ensure that light propagates along the clockwise direction and a small portion (10%) of the circulated power is spliced to the fiber patch that contains the array of Yagi-Uda nano-antennas. This ensures that not much power reaches the nano-antennas, thereby avoiding their ablation. The amount of power coupled into the nano-antenna could be increased if the antennas are placed closer to the fiber core, but at the risk of thermal damage.

Fig. 4(b) shows the relative position of the Yagi-Uda array with respect to the photodetector. Fig. 4(c) shows the emitted power at the end of the 10% arm of the 90:10 coupler as a function of the peak pump power (measured after the WDM coupler). It should be mentioned that the measurement is conducted with no external modulation of the pump source, i.e., the source is emitting continuous wave light. Also, the circulating power is 9 times higher than the power coupled to the 10% arm. Based upon the plot in Fig. 4(c), it appears that the peak power that is coupled on the fiber end is between 0 and 25 mW and the threshold pump power is about 300 mW. The emitted light is centered at the wavelength of 1091 nm.

Finally, we measure the signals coming out from the fiber end (red curve), from the Yagi-Uda nano-antennas (blue curve) and from a bare fiber (black curve), as can be observed in Fig. 5 – the plots are scaled in  $\text{dB}\mu$ , meaning that they are shown in a logarithmic scale normalized with respect to  $1 \mu\text{W}$ . For the low power signals (blue and black curves),

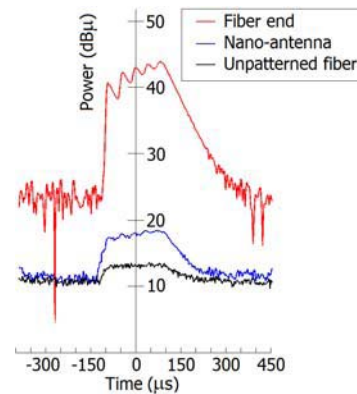


Fig. 5. Measured signals observed through a fast photodetector.

we added a seventh order digital Butterworth filter with cutoff frequency at 5 kHz. In the plots in Fig. 5, the pump power is switched on-off at a repetition rate of 2 kHz and duty cycle of 50%.

It can be clearly observed that the 3 signals have a similar shape – however, the signal at the end of the fiber is approximately 1000 times larger than the signal that can be observed laterally through a bare fiber and about 300 times larger than the signal coupled through the Yagi-Uda nano-antennas.

The distance between the Yagi-Uda array and the power meter/detector aperture is about 5 mm and the end of the fiber is placed far away (more than 20 cm) from the photodetector aperture (with respect to Fig. 4(b)) to prevent any interference with a strong signal from the fiber end. The signal being coupled through the Yagi-Uda nano-antennas could be made significantly stronger by removing a substantial portion of the fiber cladding and placing the antennas closer to the fiber core. In any case, the Yagi-Uda nano-antennas enhance the power reaching the photodetector by a factor of about 5 dB. The fast detector has an aperture with diameter of 26 mm. Powers below 10 dB $\mu$  could not be clearly observed even with filtering, meaning that the noise floor is about 10  $\mu\text{W}$  for the detector used in the experiment.

The enhancement of the evanescent fields would be maximized if the electric field were oriented along the plane of the nano-antennas and perpendicular to the axis of the Yagi-Uda antenna (e.g.  $x$ -direction in Fig. 2). This is not the case in the experiments, since the nano-antennas are placed at an angle with respect to the direction of light propagation in the core to avoid the overlapping of the signals propagating through the fiber and those coupled through the nano-antennas, i.e. the achieved enhancement could be increased. Another issue is that the fiber is cylindrical, meaning that its polarization state is arbitrary and may not lead to the highest enhancement, what could be improved by using, for example, bow-tie fibers – however our aim is to study the effect of adding arrays of Yagi-Uda nano-antennas in ordinary cylindrical fibers and their potentiality to enhance weak signals. The power reaching the nano-antennas can also be better controlled by changing the distance between the nano-antennas and the fiber core – in this sense, nano-antennas could be constructed on top of D fibers.

Finally, the arrays are arranged in such a way that individual Yagi-Uda nano-antennas are independent from each other, but they make a better use of the available space (i.e. cover almost all available area), meaning that a significant power in a certain area can be re-directed by the array.

#### IV. CONCLUSIONS

In conclusion, we have shown that the signal coming to the photodetector can be improved by a factor of 5 dB by adding directional Yagi-Uda nano-antennas that can efficiently concentrate scattered light into the photodetector and, therefore, increase the amount of power that reaches the detector – somewhat mimicking Yagi-Uda antennas that capture signals transmitted through free-space that will eventually reach our television sets.

#### REFERENCES

- [1] W. L. Stutzman and G. A. Thiele, *Antenna Theory and Design*. Hoboken, NJ, USA: Wiley, 2013.
- [2] P. Bharadwaj, B. Deutsch, and L. Novotny, "Optical antennas," *Adv. Opt. Photon.*, vol. 1, no. 3, pp. 438–383, Nov. 2009.
- [3] Z. Li *et al.*, "A plasmonic staircase nano-antenna device with strong electric field enhancement for surface enhanced Raman scattering (SERS) applications," *J. Phys. D, Appl. Phys.*, vol. 45, no. 30, p. 305102, Aug. 2012.
- [4] T. Kosako, Y. Kadoya, and H. F. Hoffmann, "Directional control of light by a nano-optical Yagi-Uda antenna," *Nature Photon.*, vol. 4, pp. 312–315, May 2010.
- [5] D. Dregely, R. Taubert, J. Dorfmüller, R. Vogelgesang, K. Kern, and H. Giessen, "3D optical Yagi-Uda nanoantenna array," *Nature Commun.*, vol. 2, Apr. 2011, Art. ID 267.
- [6] T. Dattoma, M. Grande, R. Marani, V. Petruzzelli, and A. D’Orazio, "Emission and transmission properties of a doubly resonant 3D nanodisk Yagi-Uda antenna for wireless optical communications," *Plasmonics*, vol. 8, no. 2, pp. 173–183, Jun. 2013.
- [7] J. Kim *et al.*, "Babinet-inverted optical Yagi-Uda antenna for unidirectional radiation to free space," *Nano Lett.*, vol. 14, no. 6, pp. 3072–3078, 2014.
- [8] I. S. Maksymov, I. Staude, A. E. Miroschnichenko, and Y. S. Kivshar, "Optical Yagi-Uda nanoantennas," *Nanophotonics*, vol. 1, no. 1, pp. 65–81, 2012.
- [9] A. G. Curto, G. Volpe, T. H. Taminiau, M. P. Kreuzer, R. Quidant, and N. F. Van Hulst, "Unidirectional emission of a quantum dot coupled to a nanoantenna," *Science*, vol. 329, no. 5994, pp. 930–933, Aug. 2010.
- [10] T. Shegai *et al.*, "Unidirectional broadband light emission from supported plasmonic nanowires," *Nano Lett.*, vol. 11, no. 2, pp. 706–711, Feb. 2011.
- [11] R. U. Tok, C. Ow-Yang, and K. Sendur, "Unidirectional broadband radiation of honeycomb plasmonic antenna array with broken symmetry," *Opt. Exp.*, vol. 19, no. 23, pp. 22731–22742, Nov. 2011.
- [12] A. Ahmed and R. Gordon, "Directivity enhanced Raman spectroscopy using nanoantennas," *Nano Lett.*, vol. 11, no. 4, pp. 1800–1803, 2011.
- [13] E. J. Smythe, M. D. Dickey, J. Bao, G. M. Whitesides, and F. Capasso, "Optical antenna arrays on a fiber facet for in situ surface-enhanced Raman scattering detection," *Nano Lett.*, vol. 9, no. 3, pp. 1132–1138, Mar. 2009.
- [14] E. G. Mironov, Z. Li, H. T. Hattori, K. Vora, H. H. Tan, and C. Jagadish, "Titanium nano-antenna for high-power pulsed operation," *J. Lightw. Technol.*, vol. 31, no. 15, pp. 2459–2466, Aug. 1, 2013.
- [15] FullWAVE 6.0 RSOFT Design Group. (1999). [Online]. <http://optics.synopsys.com/rsoft>
- [16] H. T. Hattori, "Analysis of optically pumped equilateral triangular microlasers with three mode-selective trenches," *App. Opt.*, vol. 47, no. 12, pp. 2178–2185, Apr. 2008.
- [17] H. Kuwata, H. Tamaru, K. Esumi, and K. Miyano, "Resonant light scattering from metal nanoparticles: Practical analysis beyond Rayleigh approximation," *Appl. Phys. Lett.*, vol. 83, no. 22, pp. 4625–4627, Dec. 2003.